Delaying the First Nucleation Event of Amorphous Solid Dispersions above the Polymer Overlap Concentration (c^*): PVP and PVPVA in Posaconazole

Sichen Song[1, 2], Xin Yao[3], Chenguang Wang[1], Changquan Calvin Sun[1], and Ronald A. Siegel[1, 4, *]

[1] Department of Pharmaceutics, University of Minnesota, Minneapolis, MN 55455

[2] School of Mathematics, University of Minnesota, Minneapolis, MN 55455

[3] Research and Development, AbbVie Inc., North Chicago, IL 60064

[4] Department of Biomedical Engineering, University of Minnesota, Minneapolis, MN 55455

* Corresponding Author: siege017@umn.edu (R.A.S.)

ABSTRACT:

A thorough understanding of effects of polymers on crystallization of amorphous drugs is essential for rational design of robust amorphous solid dispersion (ASD), since crystallization of the amorphous drug negates their solubility advantage. In this work, we measured the first nucleation time (t_0, time to form the first critical nucleus in fresh liquid/glass) in posaconazole (POS)/polyvinylpyrrolidone vinyl acetate (PVPVA) and POS/polyvinylpyrrolidone (PVP K25) ASDs and showed that the polymer overlap concentration (c^*, concentration above which adjacent polymer chains begin to contact) is critical in controlling crystallization of ASDs. When polymer concentration c is less than c^*, t_0 of POS ASDs is approximately equal to that of the neat amorphous POS, but it increases significantly when $c > c^*$. This observation supports the view that the effective inhibitory effect of crystallization in ASDs above c^* is primarily correlated with delay in the first nucleation event. Our finding is useful in efficient polymer selection and performance prediction of high drug loaded ASD formulations.

Graphical Abstract

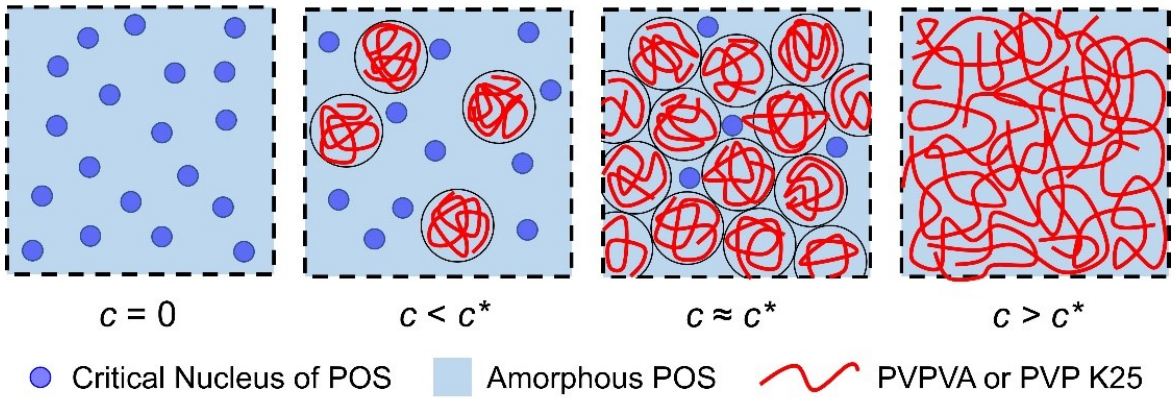

Keywords: Amorphous solid dispersion (ASD), physical stability, crystal nucleation, crystal growth, polymer overlap concentration (c^*)

INTRODUCTION

Amorphous solid dispersions (ASDs) have been an increasingly used to improve aqueous solubility and hence oral bioavailability of poorly soluble drugs.[1,2] A typical binary ASD contains an amorphous drug and a polymer. The polymer excipient in an ASD has a strong impact on its performance, including dissolution rate and supersaturation maintenance, manufacturability, and physical stability against crystallization during storage.[2-6]

Rational design of robust ASDs requires understanding the effects of polymer on the crystallization of the amorphous drug.[7-9] Crystallization includes two steps, i.e. nucleation followed by growth, with distinct kinetics.[10-14] A thorough understanding of both processes is necessary to predict overall crystallization propensity. Currently, effects of polymers on crystal growth of glass forming molecular liquids/glasses are better understood than the nucleation process.[15-19] However, nucleation kinetics have been measured in only a few multicomponent amorphous systems.[20-22]

Recently, we studied the effect of polymer concentration on crystal nucleation and growth and proposed a potential correlation between the polymer overlap concentration, c^*, (the concentration above which adjacent polymer chains begin to interpenetrate[23,24], illustrated in Scheme 1b) and the first nucleation time, t_0, (the time to form the first critical nucleus from a fresh liquid/glass).[25] Using the example of D-sorbitol/PVPs (molecular weights ranging from 4K to 55K), we showed that, in general, when polymer concentration c is less than c^*, t_0 of D-sorbitol/PVPs is approximately equal to that of the neat D-sorbitol liquid. However, when $c > c^*$, the first nucleation event is significantly retarded. At steady state, nucleation and growth rates both decrease exponentially with c, with no abrupt change occurring when $c \approx c^*$. Based on the above observations, we concluded that the effective inhibition against crystallization in binary ASDs above c^* is primarily correlated with the delay of the first nucleation event.[25-27]

In the present work, we apply the two stage (Tammann) method to investigate the role of polymer concentration c, particularly c^*, on crystallization kinetics, including the first nucleation time t_0 and steady state rate of nucleation and growth, in posaconazole (POS)/polyvinylpyrrolidone/vinyl acetate (PVPVA) and POS/polyvinylpyrrolidone (PVP K25) ASDs.[10,28] POS is a model amorphous system whose crystallization and polymorphism have been studied.[14,29] PVPVA and PVP K25 are of approximately the same molecular weight, which allows examination of the impact of variation of polymer structure on crystallization of amorphous drugs. We find that for both POS/PVPVA and POS/PVP K25 ASDs, when $c \leq c^*$, t_0s for dilute POS ASDs are identical to that of the neat amorphous POS. The value of t_0 increases gradually when $c > c^*$. Crystal nucleation and growth rates decrease exponentially against c at similar rates. Interestingly, PVP K25 provides a stronger crystallization inhibitory effect compared to PVPVA. These observations are in complete agreement with our previous results for D-sorbitol/PVPs. Our finding is relevant to the rational design of high drug loaded ASDs with minimal polymer content, which have advantages such as improving patient compliance by reducing tablet size and dosage units and lowering the cost of large scale manufacturing.

MATERIALS AND METHODS

Materials. Posaconazole (POS; form I, purity ≥ 99%) was provided by Merck. Polyvinylpyrrolidone/vinyl acetate (PVPVA) and polyvinylpyrrolidone (PVP K25) were obtained from BASF. Molecular structures and relevant physical properties of POS, PVPVA, and PVP K25 are shown in Table 1.

Table 1. Molecular Structures and Relevant Physical Properties of POS, PVPVA, and PVP K25.

	Molecular structure	M_w (g/mol)	$Đ$ (M_w/M_n)	T_g (K, onset)	T_m (K, onset)
POS	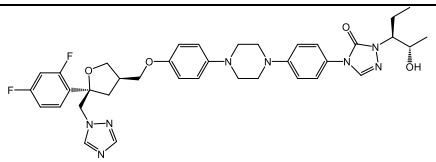	700.8	-	333.5	440.3
PVPVA	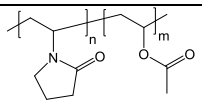	44,300	3.52	380	-
PVP K25		49,500	1.92	438	-

Sample Preparation. POS/PVPVA and POS/PVP K25 uniform physical mixtures were prepared by cryogenic milling with a Spex SamplePrep Grinder 6770 (liquid N_2 as coolant). Cryomilling was performed at 10 Hz for five 2 min cycles, each followed by a 2 min cool down. Neat POS crystalline powder, POS/PVPVA or POS/PVP K25 powder mixture was placed on a glass slide and melted at 455 K for ~2 min. A coverslip was then placed on the melt to produce a sandwiched film of ~40 μm thickness. The sandwiched liquid film was quenched to 365 K by contacting a preheated metal block.

Rheometry. Zero shear rate viscosity (η) of pure POS, POS/PVPVA, and POS/PVP K25 melts was measured using an ARES rheometer. A parallel plate geometry with diameter 25 mm was employed. Briefly, ~600 mg of powder was placed on the bottom plate after zero torque, normal force, and gap calibrations. The gap between the parallel plates was fixed at approximately 1 mm. Powder samples were melted at 448 K and equilibrated for ~3 min to guarantee complete melting before each measurement. A steady rate sweep test was performed with an initial rate of 1 s^{-1} and final rate of 100 s^{-1} with continuous N_2 purge at a flow rate of 3 standard cubic feet per minute.

First Nucleation Times. Freshly prepared pure POS, POS/PVPVA, and POS/PVP K25 thin films were held isothermally at 365 K using a Linkam LTS420 thermal stage (thermal stability ≤ 0.1 K, with dry N_2 purge to avoid moisture) for an arbitrary time (the first stage) to allow crystal nuclei to form. Then, temperature was raised to 403 K with 1-10 min hold (the second stage, no new nuclei formed) to grow nuclei into crystals with visible sizes by an Olympus BX51 polarized light microscope. This process was repeated with progressively shorter isothermal holding times in the first stage until visible crystals were not observed in the second stage. The first nucleation time t_0 was taken as the midpoint of the last two consecutive hold times (t_1 and t_2), i.e., $t_0 = (t_1+t_2)/2$. Each reported t_0 value was an average of three measurements of three separate samples ($n = 9$).

Crystal Growth Rates. Crystal growth rates of POS without or with PVPVA or PVP K25 at 365 K were measured through the thermal stage microscope (with dry N_2 purge to avoid moisture) by tracking the advance of spherulite growth fronts over time. Each reported rate was an average of 10 measurements of three separate samples. All growth rates were found to be constant over time.

Nucleation Rates. Freshly prepared sandwiched samples were stored in desiccators (0% relative humidity) at 365 K, maintained within a heating chamber (temperature stability ≤ 0.4 K) for an arbitrary observation time *t*, after which the temperature was raised to 403 K for 1-10 min, allowing nuclei to grow to a visible size and be counted. The nucleation rate was extrapolated from the nuclei density - time plot at steady state.

Solid state characterization. Differential scanning calorimetry (DSC) was performed with a TA Q1000 calorimeter in a Tzero aluminum pan with a pin hole under continuous helium purge at a flow rate of 25 mL/min. Samples (5-10 mg) were first heated from 273 to 458 K at 10 K/min to erase thermal history, quenched to 273 K, held isothermally for 2 min, and reheated at 10 K/min to 458 K. Melting point depression of POS by PVPVA and PVP K25 was evaluated from the first heating cycle, while glass transition temperatures, T_g, were measured from the second heating cycle. A Thermo DXR2 Raman microscope was used to examine the solid form. Raman scattering was excited by a diode pumped solid state laser, with a central wavelength of 532 nm. Laser power was fine tuned to 7 mW, ensuring that the sample remained undamaged while retaining spectral sensitivity. A pixel element CCD detector with an aperture size of 25 μm was employed to facilitate a resolution of roughly 3 cm^{-1} and spot size of 0.6 μm. Essential elements such as the detector, laser, apertures, and laser power underwent calibration prior to the analyses.

RESULTS AND DISCUSSION

The overlap concentration, *c, of PVPVA and PVP K25 in POS.** Before determining the overlap concentration, *c**, of PVPVA and PVP K25 in POS, it is necessary to exclude potential liquid-liquid phase separation during high temperature rheological measurements. We confirmed that POS serves as good solvent for both PVPVA and PVP K25 with favorable intermolecular interactions. This conclusion was based on a systemic depression of the liquidus temperature (T_{liq}, the lowest temperature at which a drug/polymer mixture is a completely liquid) of POS with an increasing polymer content. Figure 1 illustrates the T_{liq} depression of POS crystal (form I) doped with an increasing PVPVA concentration from neat POS (446.4 K), to 10% doped POS (443.5 K), and to 15% doped POS (441.8 K). Similar observation of POS/PVP K25 combination is shown in Figure S1.

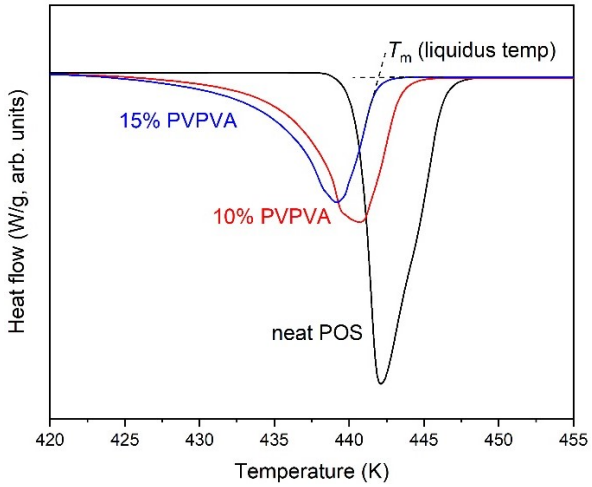

Figure 1. Melting endotherms of neat POS crystal (form I) and POS/PVPVA crystalline physical mixtures.

According to polymer solution theory, in a good solvent, polymer solutions can be roughly categorized into three regimes, i.e., dilute, semidilute, and concentrated.[23,30] In the dilute regime, polymer concentration is sufficiently low that coils are isolated from each other (Scheme 1b). Therefore, intermolecular interactions between adjacent coils are negligible, and the overall (zero shear rate) viscosity (η) of a dilute polymer solution is a linear function with respect to polymer concentration (c, wt %)

$$\eta = \eta_s(1 + c[\eta]_w) \quad (1)$$

where η_s is the viscosity of the pure solvent (small molecule drug melt) and $[\eta]_w$ is the intrinsic viscosity of the polymer/solvent combination, in unit of $\%^{-1}$. Notice that $[\eta]_w$ is slightly different from the conventional intrinsic viscosity, $[\eta]$, in that the latter is expressed as cm^3/g, based on w/v polymer concentrations.[26,30]

As the polymer concentration increases, individual polymer coils come closer and start to contact each other at the coil overlap concentration, c^*, in the semidilute regime (Scheme 1c). Hence intermolecular interactions between adjacent polymer coils start to contribute to η, leading to nonlinearity of the viscosity-composition curve. The transition between dilute and semidilute regimes occurs at c^*.[23,26,30,31] However, this crossover is not sharp since the transition between dilute and semidilute regions is not a critical phenomenon and c^* corresponds to a narrow range of polymer concentrations. Notice that c^* is generally quite small. It depends on the polymer molecular weight (M_w) according to the scaling relation $c^* \sim M_w^{-0.8}$.[23] A smaller fraction of a higher M_w polymer is needed to attain c^* by pervading the entire space. In the concentrated regime, η increases more steeply than in the semidilute regime, partially due to polymer chain entanglement (Scheme 1d) and slower polymer segmental dynamics corresponding to a higher T_g. To summarize, the c^* value (the transition between the dilute and semidilute regimes) can be estimated by identifying the crossover between linear and nonlinear portion in a viscosity – composition diagram.[26] However, there is no general equation to describe the nonlinear behavior of the $\eta - c$ curve in the semidilute and concentrated regimes.

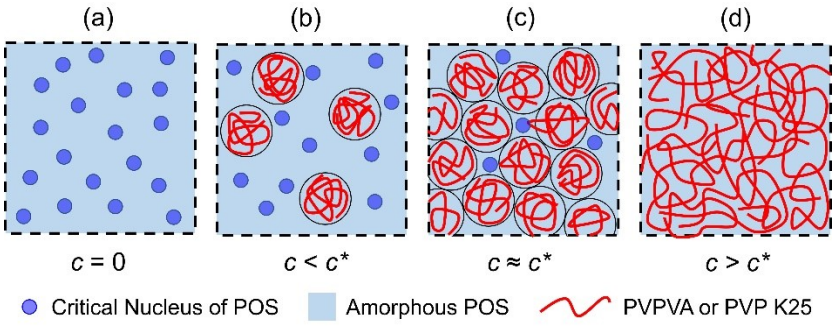

Scheme 1. Illustration of the delay of the first nucleation event in semidilute/concentrated (c-d) polymer solutions. Light blue background indicates amorphous POS serving as a good solvent, red coils indicate polymer PVPVA or PVP K25 dissolved in POS, and blue circles indicate critical nuclei of POS.

Figure 2 shows the viscosity of POS/PVPVA and POS/PVP K25 melts plotted against polymer concentration, measured at 448 K, which is approximately 8 K above T_m of POS (form I), to guarantee complete melting. When polymer concentration, c, is less than 8%, the overall viscosity η of POS/PVPVA and POS/PVP K25 melts increase linearly as a function of c. However, when c is greater than 8%, the η - c curves for both POS/PVPVA and POS/PVP K25 become nonlinear. The c^* value was determined as the transition between linear and nonlinear regions of the η - c curves, i.e., 8% for both POS/PVPVA and POS/PVP K25. Similarity of the two values of c^* may be due to the roughly comparable weight average M_w of PVPVA (44,300 g/mol) and PVP K25 (49,500 g/mol), even though the $[\eta]_w$ of PVP K25 (0.3556 $\%^{-1}$) is greater than that of PVPVA (0.2076 $\%^{-1}$).

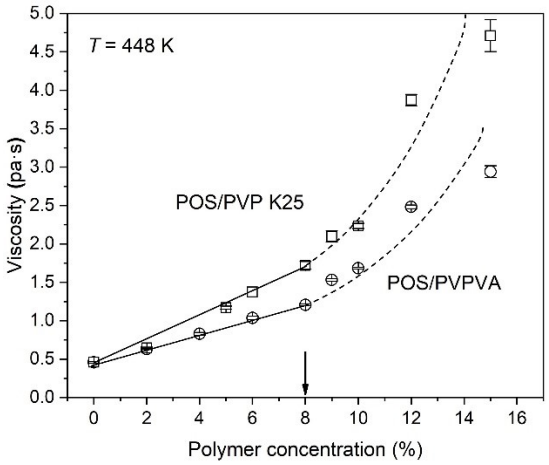

Figure 2. Viscosity-composition diagram of POS/PVPVA and POS/PVP K25 melts at 448 K. Arrows correspond to c^*, where there is a break in the slopes of the individual viscosity-polymer concentration curves.

The first nucleation time of POS/PVPVA and POS/PVP K25. In our previous article, we proposed an explanation for observations that the inhibitory effect against crystallization in ASDs only occurs when $c > c^*$.[25,26] We argued that for a dilute ASD when $c < c^*$, the presence of the pure amorphous drug domains between isolated polymer coils (Scheme 1b) permits the formation of critical nuclei in the same manner as is seen with neat amorphous drug (Scheme 1a).

Consequently, the first nucleation time, t_0, defined as the time to form the first critical nucleus (or the first group critical nuclei) of fresh amorphous solids, of dilute ASDs is approximately identical to that of the neat amorphous drug. However, when $c > c^*$, the first nucleation event can be significantly retarded due to the absence of pure amorphous drug domains (Scheme 1d). When $c \approx c^*$, retardation of the first nucleation event, or lack thereof, depends on the radius of the critical nucleus, r_c, polymer coil's radius of gyration, R_g, which depends on M_w according to the scaling law $R_g \sim M_w^{0.6}$.[24] Specifically, when $r_c << R_g$, "nooks and crannies" between adjacent polymer coils are large enough to permit crystal nuclei to form, whereas no such spaces are available when $r_c \approx R_g$.

Previously, t_0s of D-sorbitol/PVPs were determined by the one stage method (i.e. at a single temperature), since D-sorbitol spherulites exhibit relatively fast growth following nucleation. However, this method is unsuitable for systems with slow crystal growth.[10] An alternative two stage approach (Tammann's method) has been employed to determine t_0 of ASDs exhibiting fast crystal nucleation but slow growth.[10,14,28] Here, critical nuclei form without visible growth at a low temperature (the first stage) and the temperature is raised to rapidly grow the nucleus to an observable spherulite without forming new nuclei (the second stage). This two stage approach was applied to POS, whose crystals grow slowly.

Figure 3a shows examples of images used to determine t_0 values of neat amorphous POS, POS/PVPVA, and POS/PVP K25 ASDs using the two stage approach. A freshly prepared thin film sample of POS containing 15% PVPVA spent t_1 = 9000 s at 365 K (the first stage) to allow crystal nucleus to form. Then, temperature was raised to 403 K and for 8 min (the second stage, no new nuclei formed) to grow the nucleus into a spherulite with a visible size. This process was repeated with a shorter isothermal holding time t_2 = 7200 s in the first stage such that visible crystals were not observed in the second stage. The first nucleation time t_0 of 15% PVPVA/POS ASD was taken as the midpoint of the two consecutive hold times (t_1 and t_2), i.e., $t_0 = (t_1+t_2)/2$ = 8100 s.

Figure 3b plots values of t_0 for POS as a function of polymer concentration, c, for PVPVA and PVP K25, at 365 K. The t_0 values for POS/PVPVA and POS/PVP K25 are approximately identical to t_0 for neat amorphous POS when $c \leq c^*$ (8% of PVPVA and PVP K25 content), but increase gradually when $c > c^*$, as visualized by the dashed curves in Figure 3b. It is worth noting that the delay of the first nucleation event by PVP K25 is more significant compared to that by PVPVA, even though their M_ws are approximately comparable. This may be attributed to the higher T_g of PVP K25, leading to a lower segmental mobility relative to the amorphous POS.[19,32,33] Apparently the chemical structure of polymers plays an important role in controlling nucleation kinetics of ASDs.

It is worth noting that in the presence of low concentration (≤ 15%) PVPVA and PVP K25, spontaneous nucleation of POS yields the same dominant polymorph at 365 K, except for 10% POS/PVP K25. Raman mapping reveals that a new polymorph emerges alongside the dominant form within the crystal spherulite in 10% POS/PVP K25 (Figure S2). Since the presence of polymorphs does not impact the diffusion-controlled growth rate, the polymorph effect is considered negligible under this condition.

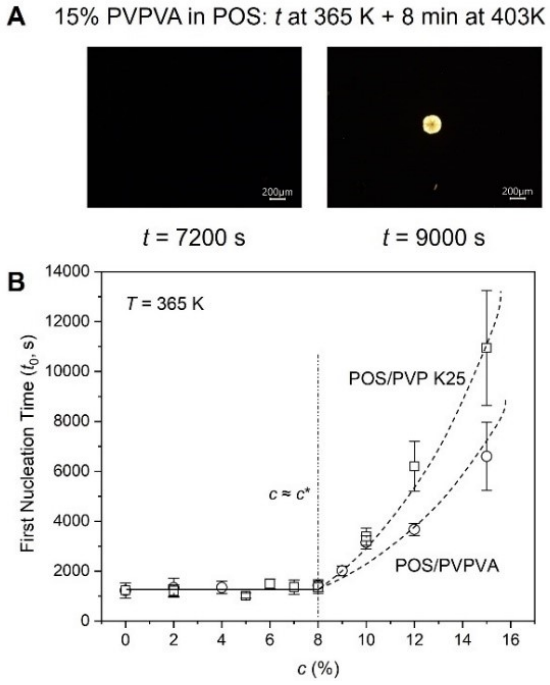

Figure 3. (a) First crystal(s) observed after POS in the presence of 15% PVPVA spent different times at 365 K (7200 or 9000 s) and then 8 min at 403 K to grow. Before heating to 403 K, no crystals were observed. (b) First nucleation time of POS/PVPVA and POS/PVP K25 as a function of polymer concentration at 365 K. Dashed curves are drawn to follow trends of increased first nucleation times with increasing polymer concentration (n = 9).

The above result mirrors those previously reported for D-sorbitol doped with relatively high M_w grade PVP K25 and K30, where the large R_g of the polymer compared to the critical nucleus radius, r_c, of D-sorbitol guaranteed enough space for the formation of critical nuclei of the amorphous drug when $c \approx c^*$, and a significant delay of the first nucleation event occurred only when $c > c^*$.[25] To further verify this phenomenon, we compare r_c of POS and R_g of PVPVA and PVP K25 dissolved in POS, at 365 K. According to classical nucleation theory (CNT), $r_c = 2\sigma/\Delta G_v$, where σ is the interfacial free energy between crystal nucleus and liquid, and ΔG_v is the bulk crystal/liquid free energy difference.[10,11,28] Also according to CNT, the crystal nucleation rate J is given by

$$J = k_J \exp(-w_c/k_B T) \qquad (2)$$

where k_J is the kinetic factor describing the attempt frequency at which molecules join the nucleus, $w_c = \frac{16\pi}{3}\frac{\sigma^3}{\Delta G_v^2}$ is the thermodynamic barrier of forming a critical nucleus assuming nuclei are of spherical shape, k_B is the Boltzmann constant, and T is the absolute temperature.[10,11,28] Huang *et al*. and Yue *et al*. have suggested that the crystal growth rate u can be used to represent the kinetic factor k_J.[10,11]

Following CNT, σ of POS can be inferred by plotting ln (J/u) vs. $1/(T\Delta G_v^2)$, using the data of nucleation and growth rates J and u with respect to temperature, as reported by Yao *et al*. (Figure 4a).[14] Figure 4b shows such a plot for POS polymorph I in bulk. Linearity of the plot indicates that the CNT can describe the data and that POS exhibits homogeneous nucleation. [Note that POS also exhibits homogeneous nucleation in the presence of PVPVA and PVP K25.

This was verified based on the stochastic nature (occurrence in the entire volume of the sample) of homogeneous nucleation. For example, 15% PVPVA/POS with a 4.7-fold sample thickness difference showed a 4.9-fold nuclei number per area under the same condition, indicating a true volume process as expected for homogeneous nucleation]. The interfacial tension between nucleus and liquid of POS, obtained by the slope of the plot, is $\sigma = 0.0123$ J/m^2.

The value of bulk crystal/liquid free energy difference ΔG_v of POS was calculated from $\Delta G_v = \Delta G/V$, where V is molar volume, obtained from the crystal densities at nucleation temperatures, and ΔG is the molar Gibbs free energy of crystallization following

$$\Delta G = \Delta H - T\Delta S \quad (3)$$

$$\Delta H = \Delta H_m - k \cdot \Delta H_m \cdot T_m \cdot \ln\frac{T}{T_m} \quad (4)$$

$$\Delta S = \Delta S_m - k \cdot \Delta H_m \cdot T_m \cdot (\frac{1}{T_m} - \frac{1}{T}) \quad (5)$$

where ΔH_m is the heat of fusion, T_m is the melting temperature, and $k = [(C_{p,L} - C_p)$ at $T_m]/\Delta H_m$, estimated as 0.003 K^{-1}.[11,34] According to the above analysis, for POS at 365 K, $\Delta G_v \approx 9.6$ kJ/mol. Therefore, $r_c = 2\sigma/\Delta G_v \approx 1.3$ nm for POS form I at 365 K.

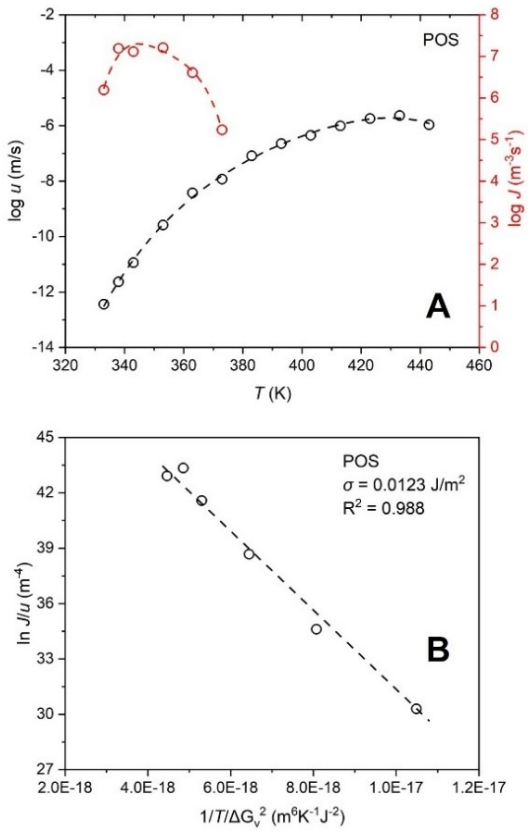

Figure 4. (a) The rate of crystal nucleation (red) and growth (black) of POS vs. temperature. Data are from Yao *et al.*[14] (b) CNT fitting for POS. ln (J/u) is plotted against $1/(T\Delta G_v^2)$. A straight line indicates that the CNT holds with a constant σ.

At present, there is no experimental data on the R_g of PVPVA and PVP K25 dissolved in POS. Nevertheless, judging from literature data on common synthetic polymers,[24] R_g of PVP K25 is estimated as approximately 15 nm according to

$$R_g = \sqrt{Nb^2/6} \quad (6)$$

where degree of polymerization, N, is approximately 446, and statistical segment length, b, is assumed to be 0.7 nm. The value of R_g of PVPVA is estimated from the relation $[\eta] \sim \frac{R_g^3}{M_w}$.[24] Therefore, $R_{g,\mathrm{PVPVA}} = R_{g,\mathrm{PVP\ K25}} \cdot \left(\frac{[\eta]_{w,\mathrm{PVPVA}}}{[\eta]_{w,\mathrm{PVP\ K25}}} \frac{M_{w,\mathrm{PVPVA}}}{M_{w,\mathrm{PVP\ K25}}} \right)^{\frac{1}{3}} \approx$ 13 nm.

Figure 5 compares the estimated R_g of PVPVA and PVP K25 and r_c of POS as a function of temperature. Due to the relatively high M_w, the R_g value of PVPVA and PVP K25 is much greater than r_c of POS across the entire temperature range. In particular, R_g is approximately twelvefold larger than r_c at 365 K. Because of the significant size difference, the amorphous POS domain between polymer coils at c^* are still large enough for the first nucleation event to occur unhindered (Scheme 1d). Consequently, the delay in the first nucleation event is observed only when $c > c^*$. The POS data mirrors the D-sorbitol/PVPs case in our previous work.[25]

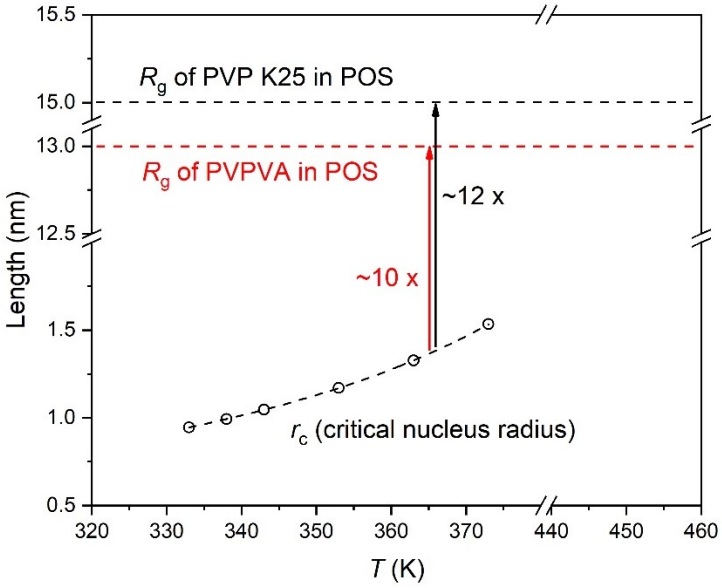

Figure 5. Relative sizes of the PVPVA or PVP K25 coil in POS vs. the critical nucleus, r_c, of POS against temperature.

Crystal nucleation and growth rates of POS/PVPVA and POS/PVP K25.

To confirm the exclusive role of c^* on the delay of the first nucleation event, the effects of polymer concentration on crystal nucleation rate, J, and growth rate, u, need to be accounted for. Figure 6a and 7a show typical data collected to measure crystal growth rate. Linearity of the POS spherulite growth distance – time plot indicates a constant growth rate. Figures 6b and 7b show typical data collected to determine crystal nucleation rates by the two-stage method. POS without and with PVPVA/PVP K25 samples were held for different times at 365 K, and then jumped to 403 K for 1-10 minutes, depending on polymer concentration (higher polymer concentration samples require longer time to grow nuclei). For example, POS containing 15% PVPVA after 70,560 s developed fewer crystals than after 163,920 s (Figure 6b). The nuclei density – time plot shows that after an induction period (lag time), a steady state is reached where the density of nuclei (counts/m^3) increases linearly with time. The slope at steady state is the nucleation rate J (counts/m^3/s).[10,28]

Figures 6c and 7c show the effect of PVPVA and PVP K25 concentration on crystal nucleation rate J and growth rate u in POS at 365 K, respectively. As polymer concentration increases, both J and u decrease at similar rates, following the relation $\log (J/u) \approx 16.0$ m^{-4}. This suggests that both nucleation and growth share the same kinetic barrier and exhibit similar molecular motions. Lodge and others proposed that the presence of polymer alters the "local viscosity" or the intrinsic effective solvent viscosity and affects the mean rotational mobility of the amorphous drug.[32,33] Yao *et al*. proposed that the nucleation rate of binary ASDs can be predicted following $J = J_0(u/u_0)$, where J_0 and u_0 are the measured nucleation and growth rates of neat amorphous drug.[20] The predicted nucleation rates at different polymer concentrations, c, based on the experimentally measured growth rate of POS/PVPVA and POS/PVP K25, are in excellent agreement with the experimentally determined nucleation rates (Figure 6c and 7c). The smooth dependence of J and u on c, both below and above c^*, for both PVPVA and PVP K25 confirms that the significant suppression of crystallization above c^* is primarily correlated with the delay of the first nucleation event, rather than steady state rate of crystal nucleation or growth. Finally, it is worth mentioning that although their M_ws are roughly comparable, the higher T_g polymer PVP K25 exhibits a stronger inhibitory effect on nucleation and growth than PVPVA, once again emphasizing the important role of polymer chemical structure on the crystallization kinetics modification.[35]

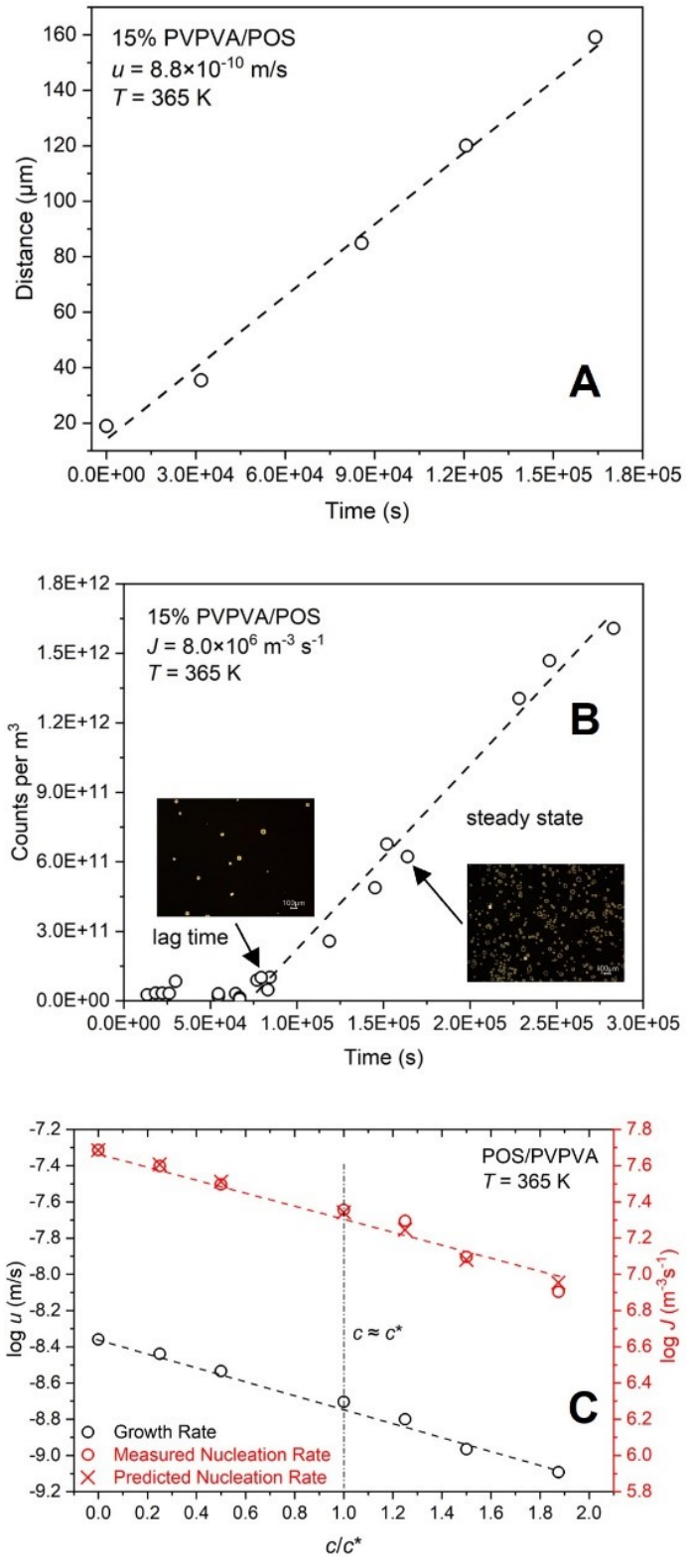

Figure 6. (a) POS crystal growth distance vs. time in the presence of 15% PVPVA, the slope is the growth rate u. (b) Two-stage method for measuring POS nucleation rate in the presence of 15% PVPVA at 365 K. The nucleation rate, J, is the slope of the nuclei density – time plot at steady state (dashed line). (c) Effect of PVPVA concentration on the steady state rates of crystal nucleation, J, and growth, u, in POS at 365 K. The errors are ± 0.1 and ± 0.4 for each reported value of log u and log J, respectively.

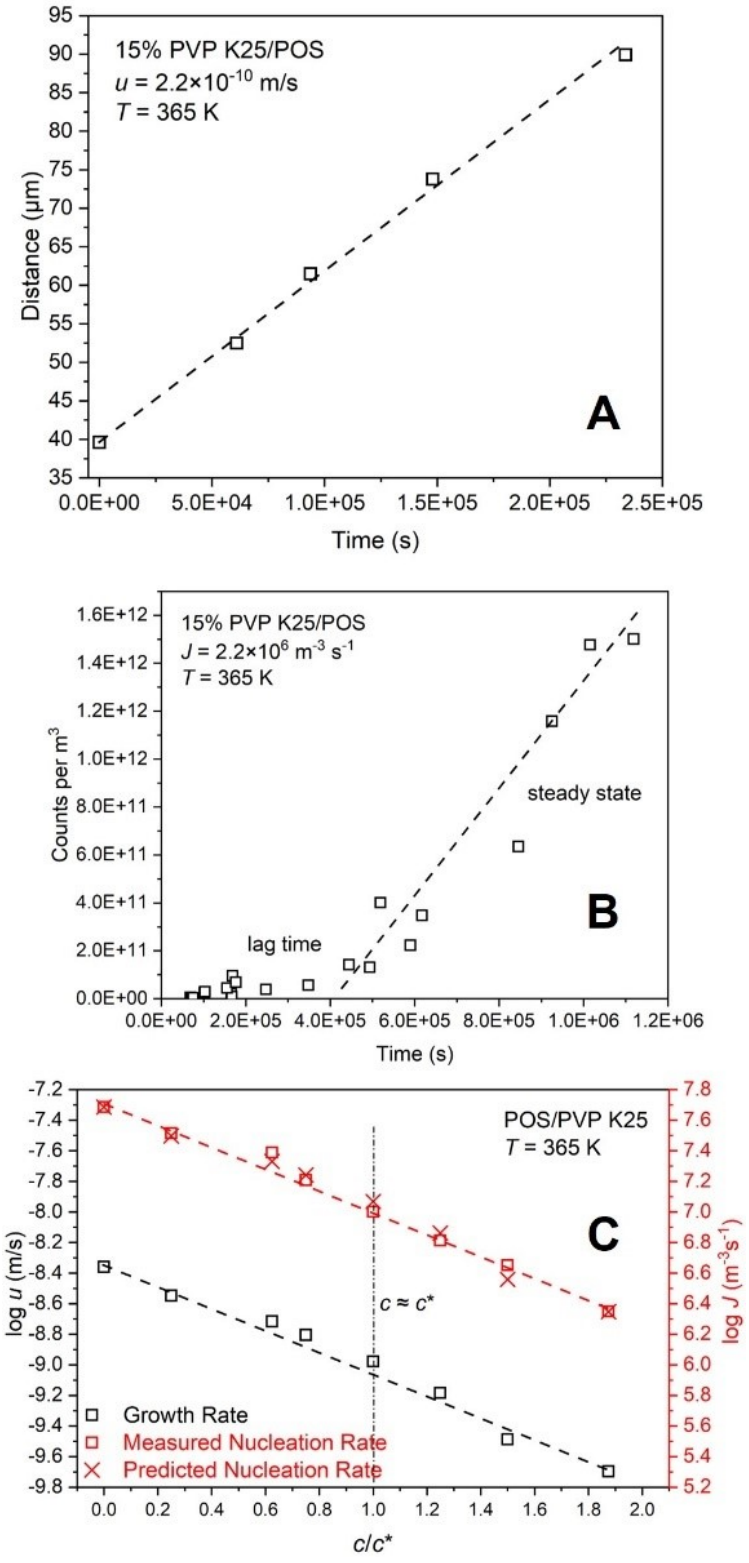

Figure 7. (a) POS crystal growth distance vs. time in the presence of 15% PVP K25, the slope is the growth rate u. (b) Two-stage method for measuring POS nucleation rate in the presence of 15% PVP K25 at 365 K. The nucleation rate, J, is the slope of the nuclei density – time plot at steady state (dashed line). (c) Effect of PVP K25 concentration on the steady state rates of crystal nucleation, J, and growth, u, in POS at 365 K. The errors are ± 0.1 and ± 0.4 for each reported value of log u and log J, respectively.

CONCLUSIONS

This work investigated the effect of polymer concentration, particularly the overlap concentration c^*, on the first nucleation time, t_0, of POS with polymer PVPVA and PVP K25. When polymer concentration c is less than or equal to c^*, t_0 of dilute POS/PVPVA and POS/PVP K25 ASDs are approximately identical to that of neat amorphous POS. When $c > c^*$, the first nucleation event is significantly delayed due to the elimination of the pure amorphous drug domain. However, no abrupt change in the dependence of steady state rate of crystal nucleation and growth can be observed on c, particularly at $c \approx c^*$. These observations argue that the effective inhibitory effect on crystallization in binary ASDs above c^* is primarily correlated with the delay in the first nucleation event. Our new results of POS ASDs are in complete agreement with the previous work of D-sorbitol/PVPs.[25] This knowledge is useful in the rational design of high drug loaded ASD formulations with sufficient physical stability against crystallization during storage. Future direction in this field will benefit from developing an effective model to predict how the local dynamics, including the first nucleation time and steady state rate of nucleation and growth of amorphous drug in an ASD, are modified relative the unmixed state.

ASSOCIATED CONTENT

Supporting Information. Melting endotherms of neat POS crystal and POS/PVP K25 crystalline physical mixtures. Raman mapping of 10% POS/PVP K25 growth rings.

Declaration of Competing Interests. The authors declare no competing financial interest.

ACKNOWLEDGMENTS

S.S. was partially supported by David J.W. Grant & Marilyn J. Grant Fellowship. Part of this work was carried out in the College of Science and Engineering Polymer Characterization and Processing Facility, University of Minnesota (UMN), which has received capital equipment funding from NSF through the UMN MRSEC program under Award Number DMR-2011401. C.C.S. and R.A.S. thank NSF for support through the Industry University Collaborative Research Center grant IIP-2137264, Center for Integrated Materials Science and Engineering for Pharmaceutical Products (CIMSEPP). Funding from Industrial Partnership for Research in Interfacial and Materials Engineering (IPRIME, UMN) is also acknowledged.

REFERENCES

1. Chiou WL, Riegelman S 1971. Pharmaceutical Applications of Solid Dispersion Systems. J Pharm Sci 60(9):1281-1302.
2. Newman A, Knipp G, Zografi G 2012. Assessing the performance of amorphous solid dispersions. J Pharm Sci 101(4):1355-1377.
3. Yu L 2001. Amorphous pharmaceutical solids: preparation, characterization and stabilization. Adv Drug Deliv Rev 48(1):27-42.
4. Serajuddin ATM 1999. Solid dispersion of poorly water-soluble drugs: Early promises, subsequent problems, and recent breakthroughs. J Pharm Sci 88(10):1058-1066.
5. Newman A, Zografi G 2022. What Are the Important Factors That Influence API Crystallization in Miscible Amorphous API–Excipient Mixtures during Long-Term Storage in the Glassy State? Mol Pharmaceutics 19(2):378-391.
6. Newman A, Zografi G 2023. Considerations in the Development of Physically Stable High Drug Load API-Polymer Amorphous Solid Dispersions in the Glassy State. J Pharm Sci 112(1):8-18.

7. Murdande SB, Pikal MJ, Shanker RM, Bogner RH 2010. Solubility advantage of amorphous pharmaceuticals: I. A thermodynamic analysis. J Pharm Sci 99(3):1254-1264.
8. Yao X, Yu L, Zhang GGZ 2023. Impact of Crystal Nuclei on Dissolution of Amorphous Drugs. Mol Pharmaceutics 20(3):1796-1805.
9. Moseson DE, Corum ID, Lust A, Altman KJ, Hiew TN, Eren A, Nagy ZK, Taylor LS 2021. Amorphous Solid Dispersions Containing Residual Crystallinity: Competition Between Dissolution and Matrix Crystallization. AAPS J 23(4):69.
10. Huang C, Chen Z, Gui Y, Shi C, Zhang GGZ, Yu L 2018. Crystal nucleation rates in glass-forming molecular liquids: D-sorbitol, D-arabitol, D-xylitol, and glycerol. J Chem Phys 149(5):054503.
11. Gui Y, Huang C, Shi C, Stelzer T, Zhang GGZ, Yu L 2022. Polymorphic selectivity in crystal nucleation. J Chem Phys 156(14):144504.
12. Wu H, Yao X, Gui Y, Hao H, Yu L 2022. Surface Enhancement of Crystal Nucleation in Amorphous Acetaminophen. Cryst Growth Des 22(9):5598-5606.
13. Yao X, Liu Q, Wang B, Yu J, Aristov MM, Shi C, Zhang GGZ, Yu L 2022. Anisotropic Molecular Organization at a Liquid/Vapor Interface Promotes Crystal Nucleation with Polymorph Selection. J Am Chem Soc 144(26):11638-11645.
14. Yao X, Borchardt KA, Gui Y, Guzei IA, Zhang GGZ, Yu L 2022. Surface-enhanced crystal nucleation and polymorph selection in amorphous posaconazole. J Chem Phys 157(19):194502.
15. Ishida H, Wu T, Yu L 2007. Sudden Rise of Crystal Growth Rate of Nifedipine near Tg without and with Polyvinylpyrrolidone. J Pharm Sci 96(5):1131-1138.
16. Cai T, Zhu L, Yu L 2011. Crystallization of Organic Glasses: Effects of Polymer Additives on Bulk and Surface Crystal Growth in Amorphous Nifedipine. Pharm Res 28(10):2458-2466.
17. Sun Y, Zhu L, Wu T, Cai T, Gunn EM, Yu L 2012. Stability of Amorphous Pharmaceutical Solids: Crystal Growth Mechanisms and Effect of Polymer Additives. AAPS J 14(3):380-388.
18. Powell CT, Cai T, Hasebe M, Gunn EM, Gao P, Zhang G, Gong Y, Yu L 2013. Low-Concentration Polymers Inhibit and Accelerate Crystal Growth in Organic Glasses in Correlation with Segmental Mobility. J Phys Chem B 117(35):10334-10341.
19. Huang C, Powell CT, Sun Y, Cai T, Yu L 2017. Effect of Low-Concentration Polymers on Crystal Growth in Molecular Glasses: A Controlling Role for Polymer Segmental Mobility Relative to Host Dynamics. J Phys Chem B 121(8):1963-1971.
20. Yao X, Huang C, Benson EG, Shi C, Zhang GGZ, Yu L 2020. Effect of Polymers on Crystallization in Glass-Forming Molecular Liquids: Equal Suppression of Nucleation and Growth and Master Curve for Prediction. Cryst Growth Des 20(1):237-244.
21. Zhang J, Liu Z, Wu H, Cai T 2021. Effect of polymeric excipients on nucleation and crystal growth kinetics of amorphous fluconazole. Biomater Sci 9(12):4308-4316.
22. Yao X, Benson EG, Gui Y, Stelzer T, Zhang GGZ, Yu L 2022. Surfactants Accelerate Crystallization of Amorphous Nifedipine by Similar Enhancement of Nucleation and Growth Independent of Hydrophilic–Lipophilic Balance. Mol Pharmaceutics 19(7):2343-2350.
23. de Gennes PG. 1979. Scaling Concepts in Polymer Physics. ed.: Cornell University Press.
24. Lodge TP, Hiemenz PC. 2020. Polymer Chemistry. 3 ed.: CRC Press.
25. Song S, Cui S, Sun CC, Lodge TP, Siegel RA 2024. Crystallization Inhibition in Molecular Liquids by Polymers above the Overlap Concentration (c^*): Delay of the First Nucleation Event. J Pharm Sci.
26. Song S, Wang C, Zhang B, Sun CC, Lodge TP, Siegel RA 2023. A Rheological Approach for Predicting Physical Stability of Amorphous Solid Dispersions. J Pharm Sci 112(1):204-212.
27. Sahoo A, Suryanarayanan R, Siegel RA 2020. Stabilization of Amorphous Drugs by Polymers: The Role of Overlap Concentration (c^*). Mol Pharmaceutics 17(11):4401-4406.
28. Fokin VM, Zanotto ED, Yuritsyn NS, Schmelzer JWP 2006. Homogeneous crystal nucleation in silicate glasses: A 40 years perspective. J Non-Cryst Solids 352(26):2681-2714.
29. Du Y, Frank D, Chen Z, Struppe J, Su Y 2023. Ultrafast magic angle spinning NMR characterization of pharmaceutical solid polymorphism: A posaconazole example. J Magn Reson 346:107352.
30. Doi M, Edwards SF. 1986. The Theory of Polymer Dynamics. ed.: Clarendon Press.
31. Daoud M, Cotton JP, Farnoux B, Jannink G, Sarma G, Benoit H, Duplessix C, Picot C, de Gennes PG 1975. Solutions of Flexible Polymers. Neutron Experiments and Interpretation. Macromolecules 8(6):804-818.

32. Schrag JL, Stokich TM, Strand DA, Merchak PA, Landry CJT, Radtke DR, Man VF, Lodge TP, Morris RL, Hermann KC, Amelar S, Eastman CE, Smeltzly MA 1991. Local modification of solvent dynamics by polymeric solutes. J Non-Cryst Solids 131-133:537-543.
33. Lodge TP 1993. Solvent dynamics, local friction, and the viscoelastic properties of polymer solutions. J Phys Chem 97(8):1480-1487.
34. Yu L 1995. Inferring thermodynamic stability relationship of polymorphs from melting data. J Pharm Sci 84(8):966-974.
35. Sahoo A, Siegel RA 2023. Drug-Polymer Miscibility and the Overlap Concentration (c^*) as Measured by Rheology: Variation of Polymer Structure. Pharm Res 40(9):2229-2237.